Calibration, validation and testing of a rotational displacement transducer for measuring wheat leaf elongation rates

Simon Dequeker†, Sarah Verbeke†, Kathy Steppe*

Laboratory of Plant Ecology, Department of Plants and Crops, Faculty of Bioscience Engineering, Ghent University, Belgium

†These authors contributed equally

*Correspondence to: Prof. Dr. ir. Kathy Steppe

Laboratory of Plant Ecology, Department of Plants and Crops, Faculty of Bioscience Engineering, Ghent University

Coupure links 653, B-9000 Ghent, Belgium

Phone +32 9 264 61 12

E-mail: kathy.steppe@UGent.be

Running head:

Rotational displacement transducer for measuring wheat leaf elongation rate

Abstract

Flag leaf growth has been emphasized in the literature as an important secondary trait for wheat breeding under drought stress. To measure leaf elongation rate (LER) in monocotyledons such as wheat, the rotational displacement transducer (RDT) has already been used in several studies, mostly on maize. Still, a comprehensive calibration and measurement protocol of the sensor is lacking. To fill this gap, several experiments were performed: (i) to calibrate the sensor and test its resilience to physical disturbances and changes in environmental conditions, (ii) to validate the calibration on growing plants, and (iii) to compare growth rate in flag leaves of well-watered and drought-treated wheat (*Triticum aestivum* L.) plants. The study showed that calibration of RDT sensors with a height gauge resulted in very accurate and robust measurements of growth rate and drought stress dynamics in monocotyledons, such as wheat. To correctly interpret the sensor measurements and derive the underlying mechanism, it is however important to consider the complex architecture of the plant, as the RDT not merely measures leaf growth, but also any potential growth of supporting parts.

Keywords: leaf elongation rate (LER), rotational displacement transducer (RDT), wheat, leaf growth dynamics, flag leaf, drought stress, plant architecture

Abbreviations:

ABA: abscisic acid
LER: leaf elongation rate
LVDT: linear variable displacement transducer
PAR: photosynthetic active radiation
RDT: rotational displacement transducer
RRT: rotation resistance transducer
VPD: vapour pressure deficit

1. Introduction

Leaf elongation rate (LER) is a major determinant of the final leaf area of monocotyledons at both the individual leaf and the whole-plant scale (Bultynck et al., 2004; Reymond et al., 2004; Chenu et al., 2008). Being representative for the amount of energy that can be captured, LER plays a prominent role in biomass accumulation and yield. At the same time, leaf growth is very responsive to environmental conditions and one of the first processes affected by changes in temperature or plant water status (Boyer, 1970; Ong, 1983; Saab and Sharp, 1989). These changes in LER as a response to sudden environmental alterations occur very rapidly (Caldeira et al., 2014) and are often transient when the environment is restored (Munns et al., 2000). While LER is affected by both water and carbon availability on a broader time scale (Lacube et al., 2017), on a shorter time scale, LER is directly associated with water relations (Coussement et al., 2018). These last authors showed that growth only occurs when turgor reaches a threshold. Below that threshold, elongation is halted, irrespective of the carbon status of the plant.

Quantifying LER continuously, in contrast to discrete, manual measurements, is necessary to study these short-term changes. This way, the underlying genotypic variation and associated mechanisms influencing LER, and ultimately yield, can be unravelled. Because drought and the associated plant stress are an increasing problem due to climate change (IPCC, 2022), understanding the physiological basis of drought-tolerant traits has the potential to identify those traits that are most relevant for better adaptation (van Eeuwijk et al., 2019) leading towards a more focused breeding approach.

Different methods exist to measure LER continuously. Rather recently, high-resolution time-lapse imaging approaches are often used, especially to measure leaf growth of dicotyledons growing not only in length but also in width (Poiré et al., 2010; Matos et al., 2014). This method has the advantage of being a high-throughput method but also the disadvantage of being processing-intensive and requiring a lot of data storage. Besides, this method is highly sensitive to distortions from surrounding leaves and plant parts and fluctuating illumination conditions (Mielewczik et al., 2013).

Therefore, for monocotyledons, where plant leaves are mainly growing in length, another method is widely used, which involves transmitting leaf elongation to a sensor, often via a pulley attached to it, which carries a thread attached to the leaf tip and a counterweight. Different sensors can be used: either a linear variable displacement transducer (LVDT) (e.g., Acevedo et al., 1971), a rotation resistance transducer (RRT) (e.g., Poiré et al., 2010) or a rotational displacement transducer (RDT) (e.g., Sadok, 2007). While the RRT is a contact sensor (i.e., a rubbing contact with a resistive element creating a voltage output), both the RDT and LVDT are contactless sensors with the advantage of wearing out less quickly, expanding their lifetime (Nyce, 2016).

The RDT sensor has already successfully been used in several experiments mainly on maize, but also on rice and *Arabidopsis thaliana*, to test the sensitivity of LER of different genotypes to evaporative demand and soil water deficit (e.g., Sadok et al., 2007; Welcker et al., 2007; Parent et al., 2010a,b) and to evaluate different hydraulic hypotheses (Caldeira et al., 2014) and the genetic architecture (Avramova et al., 2018) that underlies it. Other authors compared the diel leaf growth patterns between several monocot and dicot species (Poiré et al., 2010), tested the effects of drought and abscisic acid (ABA) on leaf growth rate (Parent et al., 2009), or examined if leaf growth and Anthesis-Silking Interval are genetically linked (Welcker et al., 2007).

Despite the widespread use of the RDT, information on its operation, calibration and use remains limited. In this regard, the lion's share of studies refers to Sadok et al. (2007), which was the first study applying this sensor. Although Sadok et al. (2007) checked some features and possible pitfalls, such as the potential influence of the applied weight on LER and whether temperature and vapour pressure deficit (VPD) had an effect on the thread extensibility, there seems to be no protocol on sensor calibration and use. Moreover, note is rarely taken of the fact that the RDT does not purely measure leaf growth, but also, if present, the growth of structures supporting the leaf, i.e., its leaf sheath and subsequent internodes. With most studies using RDT on the sixth to eighth leaf of maize, the growth of supporting structures is almost absent. However, when measuring leaves at a different stage or of a different monocotyl, or when measuring on other organs, such as silks (Turc et al., 2016), there is a danger of overlooking the growth of the supporting structures.

To increase knowledge of a sensor with which much research has already been done, but has not yet intensely been tested, three experiments were conducted. In the first experiment, the sensor was calibrated and tested for changing environmental conditions and for robustness against disturbances. In the second experiment, the calibration method was validated on growing wheat leaves, without taking into account plant morphology. As cereal flag leaves take a central role in the process of grain filling, but understanding of flag leaf physiology and morphology under drought is critically lacking (Biswal et al., 2013), the third experiment consisted of a drought treatment on wheat plants. This was to determine to which extent flag leaf support structures in wheat contribute to the measured leaf growth, whether water deficit alters this contribution, and the extent to which drought stress drives wheat flag leaf growth dynamics.

2. Materials and methods

2.1 Experiment 1: Setup and calibration of RDTs and testing their performance in different environmental conditions

Eight rotational displacement transducers (RDTs; 601-1045 Full 360° Smart Position Sensor; Spectrol Electronics Ltd, Swindon, UK), fixed to a metal frame 1.5 m above table beds, were attached to a 3D-printed pulley (diameter 29.81±0.46 mm), which carried a Kevlar (Paracord, the Netherlands) thread fixed to a 20 g counterweight (Figure 1). The Kevlar thread was selected from a screening experiment and chosen for its properties: low stretch, thin, flexible and enough grip so the thread does not slip on the pulley. The sensors were connected to a data logger (CR1000 and AM16/32 Multiplexer, Campbell Scientific, Logan, UT-US) and data was collected in the PhytoSense software (Plant AnalytiX, Mariakerke, Belgium) every min and then averaged over 10 min. All experiments were conducted in a fully controlled growth chamber (WEKK 10.40.8L SN 40816000381001, Weiss Technik, Reiskirchen-Lindenstruth, Germany).

Each sensor was calibrated by fixing the loose end of the Kevlar thread to a digital height gauge (Schut Geometrical Metrology, the Netherlands; measuring range 0-600 mm; resolution 0.01 mm). Six calibration values within one revolution of the pulley and six continuous full rotations per sensor were obtained. As only the change in displacement, and not the absolute height of the gauge is related to the sensor output, the change in height was plotted against the change in sensor output for each rotation. This procedure was repeated under changing environmental conditions (set air temperature of 15°C, 20°C and 25°C and relative humidity of 63% and 83%) and an inclined position of the height gauge in relation to the pulley (gauge 12 cm away from the central position, which is perpendicular below the pulley). Also, a theoretical calibration was performed based on the maximum voltage difference and the circumference of the pulley of each sensor.

To test whether altering environmental conditions affect the performance of the sensor system (logger + RDT + pulley + Kevlar thread) (Sadok et al., 2007) in absence of biological material, the thread of all sensors was attached to a metal bar for 40-60 hours. As a first treatment, to test extreme conditions, air temperature was reduced stepwise from 20°C to 0°C, -5°C and finally -10°C where the temperature at each step was held constant for 6h. As a result, relative humidity rose from 60% to 85%. In a second treatment, temperature was set to simulate a realistic daily variation on the sensor system with a day/night cycle of 14 h/ 10 h where daytime temperature was set at 22°C and night-time temperature at 17°C. Relative humidity then varied between 65 and 86%. In both treatments, the cycle was repeated twice.

2.2 Experiment 2: validation of the sensor calibration on wheat plants

For the second experiment, wheat seeds (*Triticum aestivum* L. cv. Servus) were disinfected before sowing by subsequently immersing them 2 min in 70% ethanol and 10 min in 20% bleach and finally rinsing the seeds with distilled water. On February 7, 2022, the seeds were sown in eight 4 L pots (10 seeds per pot) filled with equal amounts of commercial potting mix (AVEVE, Leuven, Belgium: DM 20%, pH 4.5-7, EC 75 mS.m^{-1} with NPK fertilizer 14-16-18: 0.5 kg.m^{-3}) at a depth of 3 cm and irrigated immediately with 600 mL water. Seed germination was around 70%. Artificial lights (T5 Reflex Cool White, Philips, Eindhoven, Netherlands) in the growth chamber were switched on during a 14 h light period from 10 a.m. to midnight. During the first four weeks, PAR (photosynthetic active radiation) intensity of the lamps was set to 150 µmol.m^{-2}.s^{-1}. After four weeks this was increased to 400 µmol.m^{-2}.s^{-1}. Photosynthesis is at 70% of the light saturation at this level (based on light response curves measured on the flag and penultimate leaves measured at 0, 100, 250, 500, 1000, 1500, 2000 µmol.m^{-2}.s^{-1}; n=70). The temperature was set to 17°C during the night and 22°C during the day. Relative humidity was set at 60%, but data showed that it reached 65% during the day and 80% during the night. Plants were watered 250 mL three times a week.

Relative humidity and temperature were measured with two RH/T sensors (type EE08, E+E Elektronik, Engerwitzdorf, Austria). PAR was measured with two quantum sensor (SQ-110-SS, Apogee Instruments, Logan, UT-US) and atmospheric CO_2 concentration was monitored with a carbon dioxide probe (CARBOCAP GMP343, Vaisala, Vanha Nurmijärventie, Finland). All environmental sensors were placed at the height of the canopy in between the plants. Data were logged every 2 min with a data logger (CR1000 and AM16/32 Multiplexer, Campbell Scientific, Logan, UT-US) and collected and stored in the PhytoSense software (Plant AnalytiX, Mariakerke, Belgium).

To validate the calibration performed with the height gauge on plants, the tips of wheat leaves (trefoil stage) were connected to the Kevlar threads with fabric sewing clips (Wonderclips), making sure that the point of attachment was perpendicular below the pulley (Figure 1). Random plants were selected from the eight pots for this purpose. Four validation measurements were conducted for each sensor (n=4), comparing RDT measurements with manual measurements of leaf growth: at two time points (2-6 days in between), height of the attached fabric clips was read via a ruler inserted into the soil next to the wheat plant, thereby not disturbing the sensor. Between measurements, the growth chamber was not entered and when leaf growth was less than 8 cm, the data point was removed to avoid noise, which was higher on slow growing leaves. The loggers of two sensors failed several times, eventually leaving three sensors with three repetitions and one sensor with two repetitions.

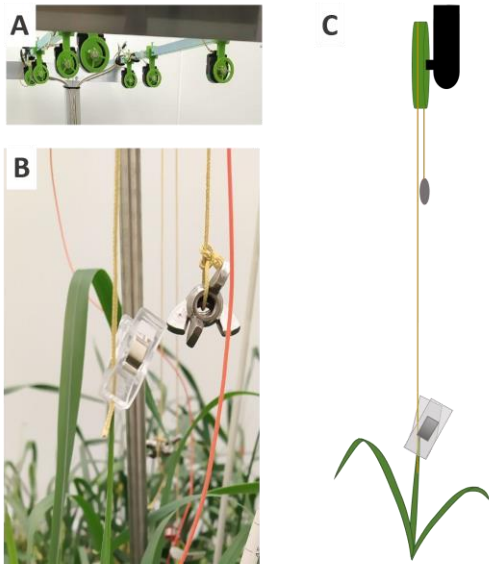

Figure 1. Experimental setup of the RDT sensor. A) RDT sensors with their 3D-printed pulleys (in green), fixed to a metal frame. B) Attachment of the Kevlar thread to a leaf with a fabric sewing clip (Wonderclip). The other end is attached to a counterweight. C) Schematic representation.

2.3 Experiment 3: measuring growth rate of wheat flag leaves under drought stress

For the third experiment, 42 pots were sown on April 25, 2022, in the same way as explained for experiment 2. A different potting mix was used (DCM, Grobbendonk, Belgium: DM 30%, pH 4.5-7, EC 35 $mS.m^{-1}$ with NPK fertilizer 7-7.5-8: 1.5 $kg.m^{-3}$). The plants were watered every two days up to a soil moisture percentage of 35-40% (field capacity) (measured with a moisture sensor: SM 300 Moisture Sensor and HH2 Moisture Meter, Delta-T Devices, Cambridge, UK). On June 30, one day before the measurements started, plants were randomly divided into two groups. Drought-treated plants (n=150) and control plants (n=150) now received 150 mL and 500 mL of water every two days, respectively, to reach a soil moisture level of 20-25% and 35-40%, respectively. Once, on July 8, drought-treated plants received 300 mL to avoid excessive drought stress and cessation of leaf elongation. Plants were always watered before the lights in the growth chamber were turned on (i.e., before 10 a.m.). The drought experiment lasted for 14 days and included flag leaf emergence, which occurred on July 13 (79 days after sowing) and

July 10 (76 days after sowing) for the control and drought treatment, respectively. Flag leaf emergence was noted when the ligule of the flag leaf was visible in 50% of the plants. On June 30, 2022, four plants (from four different pots) out of each treatment were selected where the emerged part of the flag leaf was smaller than 8 cm, to keep biological variation in phenology as small as possible. These flag leaves were connected to the RDTs as described previously (Figure 1). On several days, the length of the emerged flag leaf was measured manually with a ruler, for validation purposes. These measurements differed from the length measurement in experiment 2 in the sense that not the distance from the soil to the leaf tip was measured, but only the length of the emerged part of the flag leaf (first only blade and then blade + sheath as soon as visible).

From the remaining 17 pots in both treatments, plants whose emerged part of the flag leaf was smaller than 12 cm were selected and marked on June 30, 2022. As not enough plants were available with an emerged part of the flag leaf smaller than 8 cm, this threshold was increased to 12 cm. These plants were used for destructive organ lengths and water potential measurements. The lengths of the flag leaf blade and flag leaf sheath were measured with a ruler. Water potential was measured with a Scholander pressure chamber (model 600, PMS Instrument Company, Albany, OR-USA) at predawn (between 8 and 10 a.m.) and during the day (between 2:30 p.m. and 4 p.m.) in the flag leaf, immediately after cutting the leaf. Both predawn and daytime measurements were taken in the first week of the experiment (i.e., on July 1, 3, 5 and 7) the day before watering. When the flag leaf was almost fully emerged, water potential was measured again on July 12 (at predawn) and on July 14 (during day).

2.4 Data analysis

The data was processed and visualized in R. To test the effect of environmental conditions on the calibration, and to check whether a sensor-specific calibration is necessary, a multiple linear regression was performed:

$$\Delta gauge = \Delta rdt + sensor + rotation + T + RH + position + position * rotation \quad (1)$$

whereby $\Delta gauge$ (mm) is the linear displacement of the gauge and Δrdt (mV) is the change in sensor output. $sensor$ is a nominal variable that indicates each sensor and $rotation$ an ordinal variable that indicates the consecutive full rotation of the pulley. This variable was added to check whether the length of the thread between the pulley and point of attachment significantly affected the calibration. T (temperature: 15.6°C, 20.6°C and 25.6°C), RH (relative humidity: 63% and 80%) and $position$ (central, angled and angle corrected) were also included as variables in the regression analysis.

To calibrate the sensors, a sensor-specific calibration was performed, using a linear regression analysis. Only data where the gauge was placed perpendicular below the pulley were included:

$$\Delta gauge = \beta . \Delta rdt \quad (2)$$

3. Results

3.1 Sensor calibration and performance

Multiple regression analysis (adjusted R^2=0.9996, df=1435) showed that a sensor-specific calibration was necessary (Table 1). Environmental conditions had no significant effect on the calibration, nor did an increasing number of rotations when the gauge was positioned perpendicular below the pulley. When the gauge was positioned at an angle, however, the calibration was significantly influenced (p=0.00519). This effect increased with each rotation (p=$5.25*10^{-7}$), which was due to the triangulation, where the angle of the inclination decreased as the gauge moved upwards. Correction for this error by taking triangulation into account neutralised this influence (p=0.1382 and p=0.7005 for the influence of the position alone and the correlated effect of the position with the number of rotations; Table 1, Figure 2). This means that the inclined position did not cause any additional slip of the thread. Calibration values for each sensor were then calculated with separate regression analyses (Table 2). Theoretical calibration values, as calculated from the circumference of the pulley and the maximum voltage difference on the transducer, resulted in a consistent underestimation of the calibration values (Table 2) and would thus result in an underestimation of the displacement difference.

Table 1. Multiple regression analysis (Eq. 1) of the calibration experiment. Coefficients are depicted with standard error. Significance levels: * p < 0.05, ** p < 0.01, and *** p < 0.001.

	Estimate			Unit	p-value	
(Intercept)	-0.1221	±	0.1746	mm	0.4843	
ΔRDT	0.0220	±	0.0000	$mm.mV^{-1}$	~0.0000	***
Sensor 2	0.0344	±	0.0496	mm	0.4881	
Sensor 3	-0.2200	±	0.0499	mm	1.09E-05	***
Sensor 4	-0.6021	±	0.0498	mm	3.95E-32	***
Sensor 5	0.3199	±	0.0496	mm	1.59E-10	***
Sensor 6	-0.1926	±	0.0496	mm	1.09E-04	***
Sensor 7	-2.1685	±	0.0502	mm	9.76E-262	***
Sensor 8	0.2355	±	0.0493	mm	1.94E-06	***
RH	0.0034	±	0.0021	$mm.\%^{-1}$	0.1008	
T	0.0043	±	0.0043	$mm.°C^{-1}$	0.3238	
position - angled	0.2181	±	0.0779	mm	5.19E-03	**
position - angle corrected	0.1155	±	0.0779	mm	0.1382	
rotation	0.0006	±	0.0090	$mm.rotation^{-1}$	0.9493	
position - angled*rotation	0.0980	±	0.0194	$mm.rotation^{-1}$	5.25E-07	***
position - angle corrected*rotation	0.0075	±	0.0194	$mm.rotation^{-1}$	0.7005	

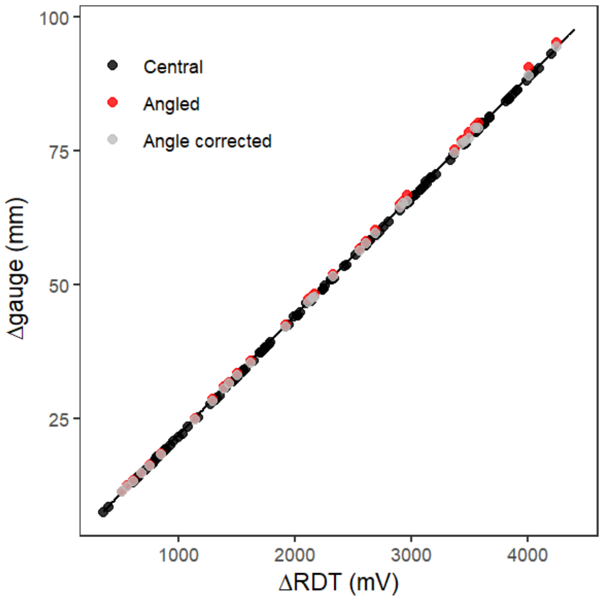

Figure 2. Example of the calibration for sensor 1. Different vertical positions of the gauge in relation to the sensor are depicted. When the gauge is not positioned vertically below the sensor ('Angled'), correction for trigonometry is necessary ('Angle corrected'). The blackline represents the calibration (Table 2) of that sensor.

Table 2. Calibration coefficients with standard error. Coefficients were calculated with a linear regression analysis (Eq. 2) for each sensor separately. The theoretical calibration was based on the circumference of the pulley. Only data with the gauge positioned vertically below the sensor was included in the regression analysis. All coefficients were highly significant ($p < 1\times10^{-224}$).

	Coefficient (mm.mV^{-1})			
	Regression			Theoretical
Sensor 1	0.022195	±	1.25E-05	0.021184
Sensor 2	0.022147	±	1.80E-05	0.021177
Sensor 3	0.022045	±	2.53E-05	0.021018
Sensor 4	0.021865	±	1.30E-05	0.020929
Sensor 5	0.022096	±	1.19E-05	0.021087
Sensor 6	0.021814	±	1.77E-05	0.020919
Sensor 7	0.021017	±	1.75E-05	0.020135
Sensor 8	0.022079	±	1.41E-05	0.021206

Environmental conditions (T, RH and VPD) impacted the sensor system performance (logger + sensor + pulley + Kevlar thread), but this impact depended on the extremity of conditions (Figure 3). In the first treatment, where air temperature was stepwise brought below zero (Figure 3A) and VPD was changing from over 1 kPa to near zero (Figure 3C), not all sensors followed the same pattern: some sensors showed a negative deviation, others a positive one. One sensor (sensor 3) turned out to be much more sensitive to environmental shocks (maximum deviation 14.21 mm, not shown), increasing the average deviation. The maximum deviation of the second most sensitive sensor (sensor 4) was only 1.09 mm. In the second treatment, where changes in environmental conditions were less severe, representing a more standard day (Figure 3B), all sensors followed the VPD pattern to a lesser or greater extent (Figure 3D). The maximum deviation of an individual sensor was 0.63 mm. The two sensors found to be the most sensitive were the same in both treatments.

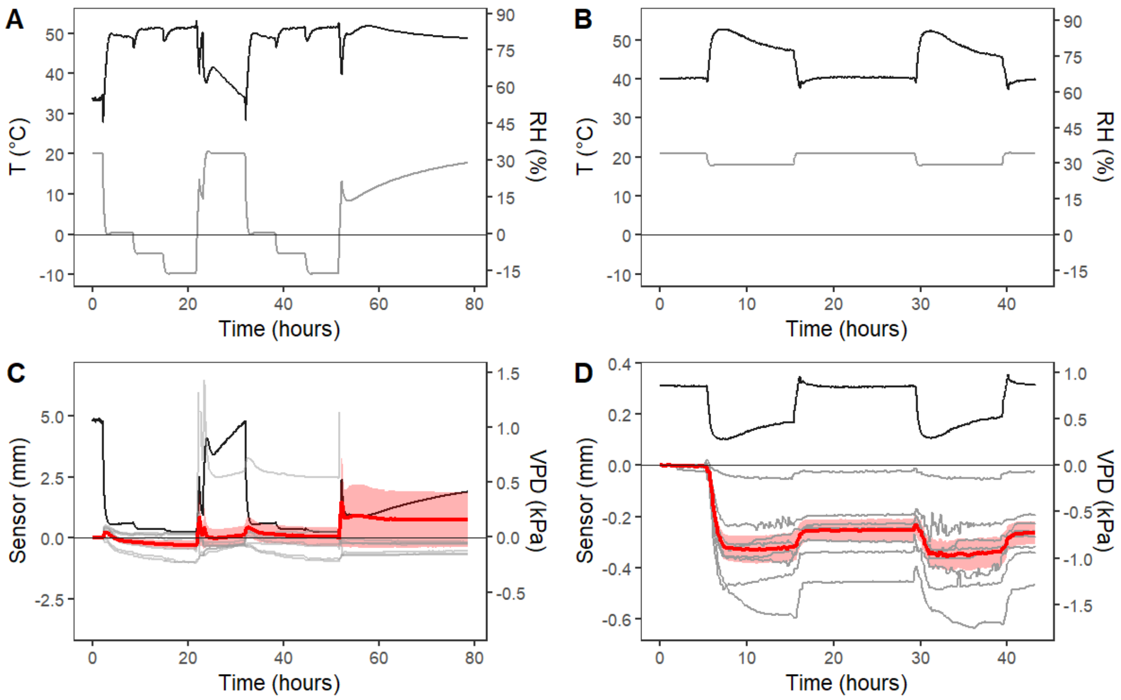

Figure 3. Displacement registered by the RDT sensors due to changing environmental conditions. The sensors were attached to an immobilised metal rod. A) and B) show the change in relative humidity (black top line) and temperature (grey bottom line) during two treatments. C) and D) show the change in VPD (black line) and sensor displacement (grey lines represent individual sensors and the red line and band the mean deviation and standard error, respectively, of all eight sensors). In C) some data of one sensor (sensor 3) is not depicted as the axis limits were set to optimise visualisation.

3.2 Sensor validation and robustness

When wheat leaves were growing undisturbed (i.e., the growth chamber was not entered), manual measurements of leaf growth matched well with RDT measurements (Figure 4), which is illustrated by a high R^2-value (0.99). Even when sensors were disturbed, by experimental handling, this had relatively little impact on the performance of the RDT sensors (Figure 5). The first ‘series of disturbances’ (red dots in Figures 5A and B), included installation of another sensor on the measured leaves, shortening the Kevlar threads, manual measurements with a ruler and performing two rounds of destructive measurements on surrounding plants. A second series of disturbances (red dots in Figures 5B and D) included again manual measurements with a ruler and destructive measurements on surrounding plants, complemented by measurements of the moisture percentage of the soil in the pots. In all these cases, the Kevlar threads were touched and moved or were likely to have been at some point. While a few disturbances can be detected in a sensor (outliers in red dots in Figure 5), these disturbances are filtered out when averaging multiple sensor data.

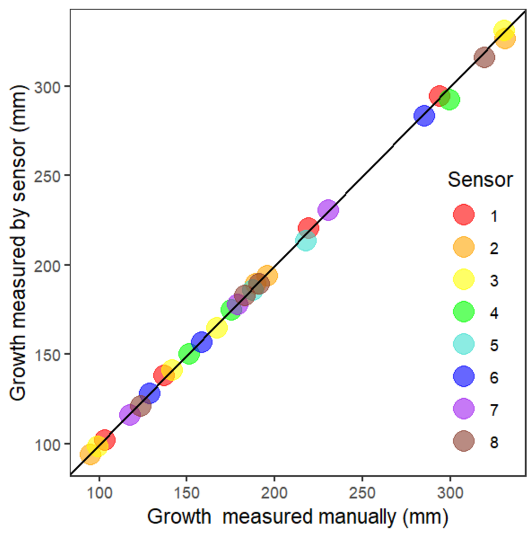

Figure 4. Relation between measurements of leaf growth with RDT sensors and manual measurements with a ruler ($R^2 = 0.99$). Each sensor has a different colour. The black line indicates a 1:1 relationship.

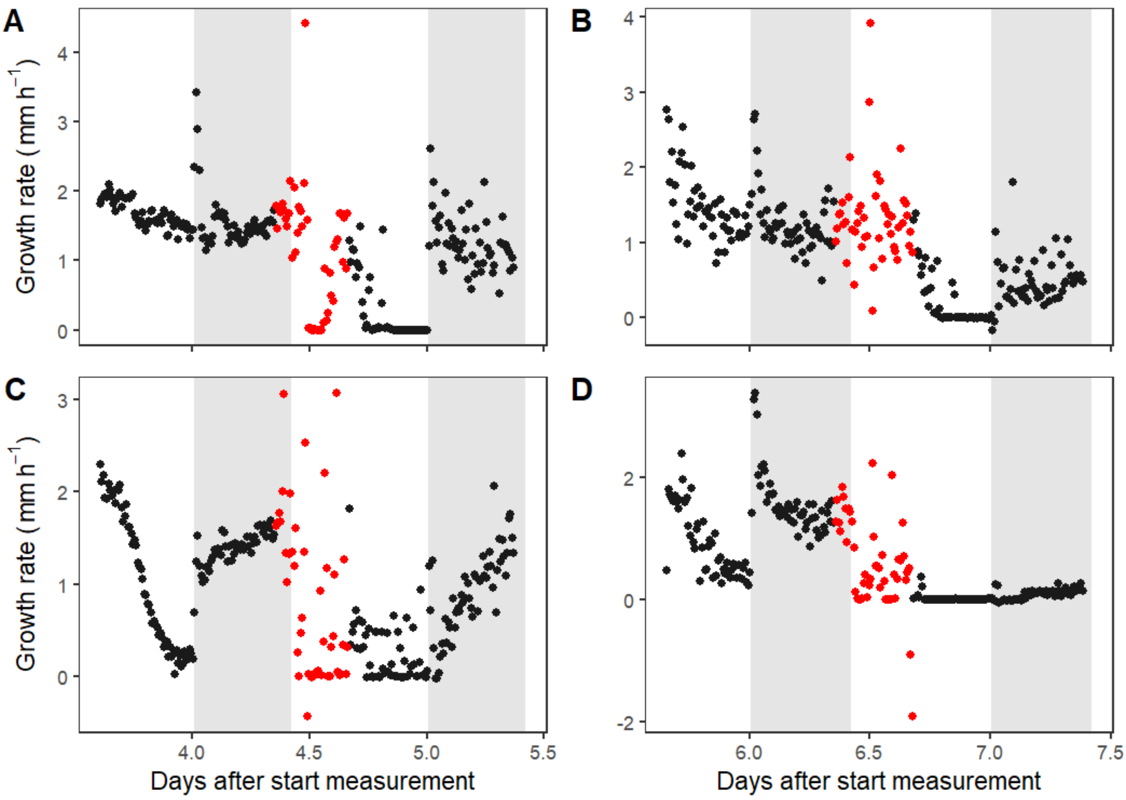

Figure 5. Growth rate of a wheat flag leaf measured with a RDT sensor during periods when the growth chamber was not accessed (black dots) and periods when the growth chamber was accessed, and the measurement process potentially disrupted (red dots). A) and B) well-watered plant, C) and D) drought stressed plant. Red dots in A) and C) were obtained when installing other sensors on the leaves, shortening the Kevlar threads, conducting manual measurements with a ruler on RDT-attached leaves and two rounds of destructive water potential measurements on surrounding plants. In a second period (red dots in B and D), manual measurements with a ruler and destructive water potential measurements on surrounding plants were conducted and the moisture percentage of the soil in the pots was measured. Grey areas indicate the absence of light conditions.

3.3 Wheat flag leaf growth and the effect of drought stress

Drought stress was imposed on half (n=4) of the plants monitored with the RDT. Predawn water potential was measured in the flag leaves on the days after irrigation in the first week and was -0.59 ± 0.32 MPa and -1.07 ± 0.61 MPa, for the well-watered and drought-treated plants, respectively (n=20). During daytime conditions, water potential in watered and drought-treated flag leaves decreased to -1.04 ± 0.25 MPa and -1.29 ± 0.18 MPa, respectively (n=20), demonstrating a slight, but not extreme drought stress in the drought treatment.

Flag leaves of drought-treated plants elongated on average 64% less than flag leaves of well-watered plants (22.2 ± 6.5 cm versus 34.8± 5.2. cm, respectively) (Figure 6). Over half (61.3%) of that growth difference was established during the first three measurement days. Dissection and measurements of well-watered sampled plants showed that there was little growth of the flag leaf blade after the first three days of measurement whereas flag leaf sheath growth was present throughout the experiment, but less so during the first three days (Figure 7).

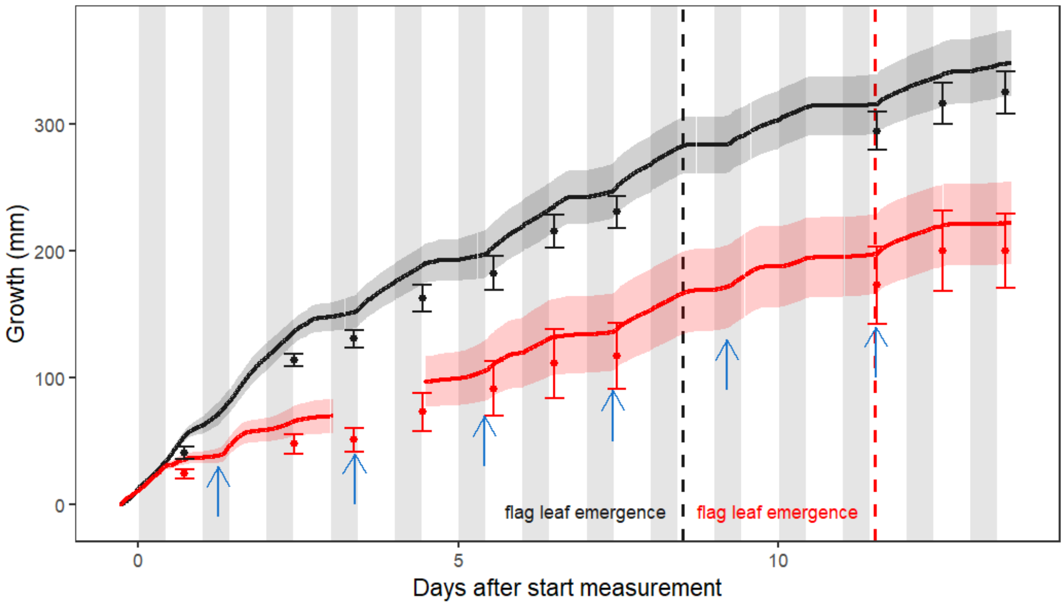

Figure 6. Growth of wheat flag leaves (blade + sheath) of well-watered plants (black, n = 4) and drought-treated plants (red, n = 4). Lines indicate average flag leaf growth as measured by the RDT sensor, error bands indicate standard error and dots show growth as manually measured, with standard error (n = 4). Blue arrows represent the times of watering. Control and drought-treated plants received 500 mL and 150 mL, respectively, each time, except for day 8, when drought-treated plants were watered 300 mL to avoid wilting. The black and red vertical dashed lines indicate the moment when 50% of the flag leaves of well-watered plants and drought plants, respectively, were fully emerged, respectively. Grey areas in the background indicate the absence of light.

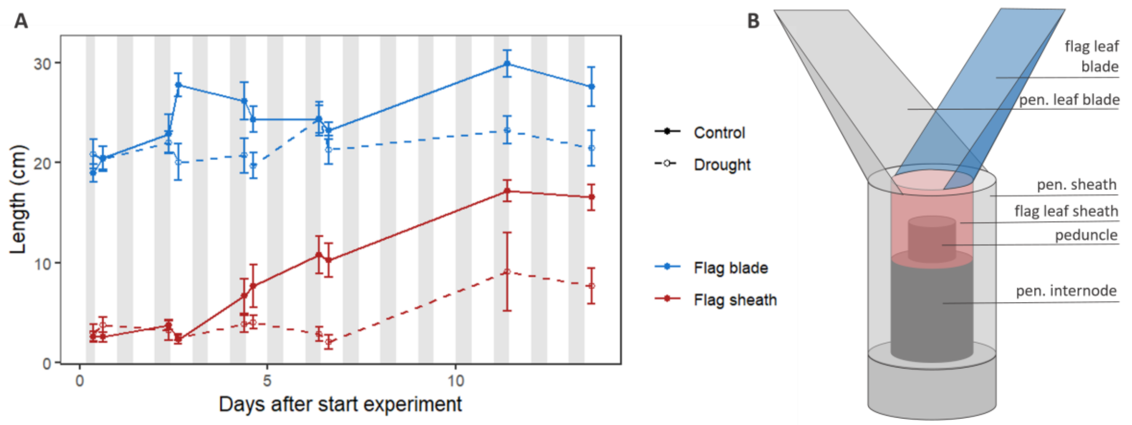

Figure 7. Growth of the flag leaf blade and sheath during the experiment (A). These destructive measurements were performed on other plants that the monitored plants. Average organ length (n = 5) with standard error is depicted, with lines to emphasize the trends over time. Full circles and lines represent the control treatment, while empty circles and dashed lines represent the drought treatment. Grey areas in the background indicate the absence of light. B) Schematic representation of the leaf morphology in the same colours depicted in graph A. Pen: penultimate.

Drought affected leaf elongation. At the start of the experiment the flag leaf blade of the drought-treated plants was on average 1.88 ± 5.32 cm (n = 5) longer than of well-watered plants. The leaf sheath was the same in both treatments at the beginning of the experiment (difference of 0.38 ± 3.02 cm, n = 5). However, final leaf blade and leaf sheath of the drought-treated plants were, respectively, 6.22 ± 8.38 cm (n = 5) and 8.88 ± 6.91 cm (n = 5) shorter than well-watered plants.

Referring to Figure 6, there is a significant difference between the manual measurements and the sensor data. Manual measurements indicated less flag leaf growth compared to RDT measurements for both drought (-9.7%) and well-watered (-6.4%) plants. The difference in measured growth between these two measurement methods (manual – RDT sensor) was mainly established during the first three days of the experiment (Figure 8). Since the manual measurements were discrete, the same discrete intervals were used for the RDT sensor data. Negative values indicate a slower growth rate of the manual measurements compared to the RDT data. After three days, the difference in measured leaf growth between the two methods disappeared and both methods measured equal growth rates. Figure 8 also shows that the overestimation of the RDT sensors during the first days did not differ under drought stress conditions.

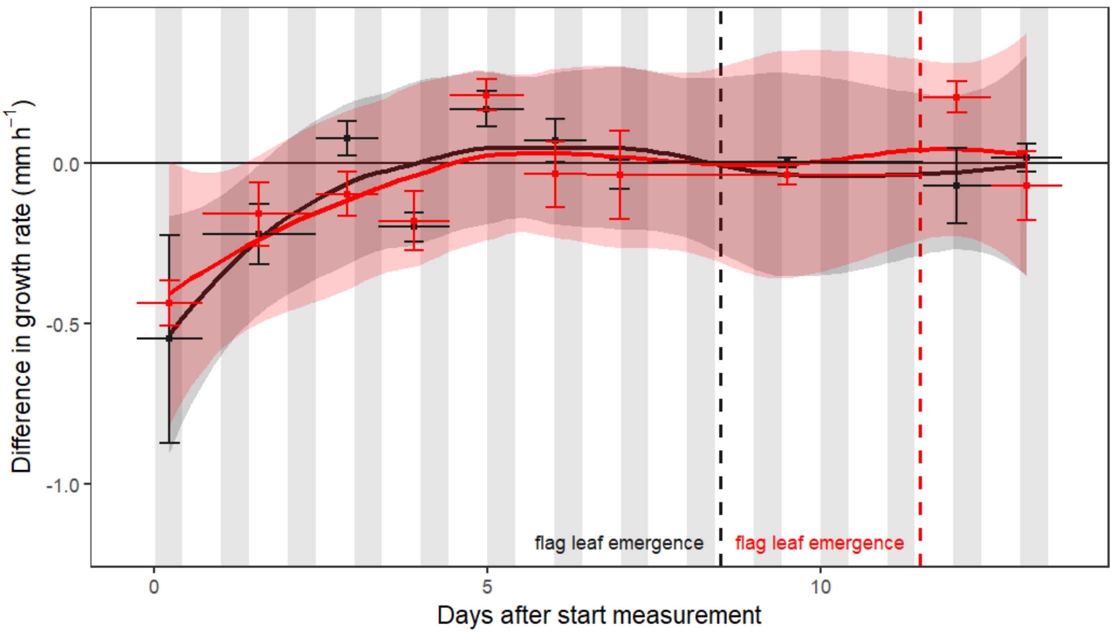

Figure 8. Difference in growth rate between the manual and RDT sensor measurements in well-watered plants (black dots) and drought-treated plants (red dots). This difference was calculated by subtracting RDT growth rates per hour from manual measurements. Vertical lines through the dots represent the standard error, the horizontal lines through the dots represent the time period for which the growth rate was calculated. Trend lines were added in R (function geom_smooth). Vertical black and red dashed lines show the moment when 50% of the flag leaves of well-watered plants and drought-treated plants were fully emerged, respectively. Grey areas in the background indicate the absence of light.

Figure 9 shows the continuous pattern of the growth rate, which is only possible to display when using RDT sensors. It shows that the water regime had a major impact on daily growth dynamics of wheat flag leaves. Immediately after watering, growth rate of both drought and well-watered plants increased, which was more pronounced in the well-watered plants. On the day before watering, growth rate declined, but this was more pronounced and earlier for drought-treated plants where the growth rate more often declined to zero compared to well-watered plants. The night following a watering event, growth rate of drought-treated plants increased. Both drought-treated plants and well-watered plants reached their maximum growth rate just before lights were switched on. On the second day after watering, the growth rate of well-watered plants also stalled, often keeping pace with the drought-treated plants. This suggests that the well-watered plants were also suffering mild water deficit on the second day after watering.

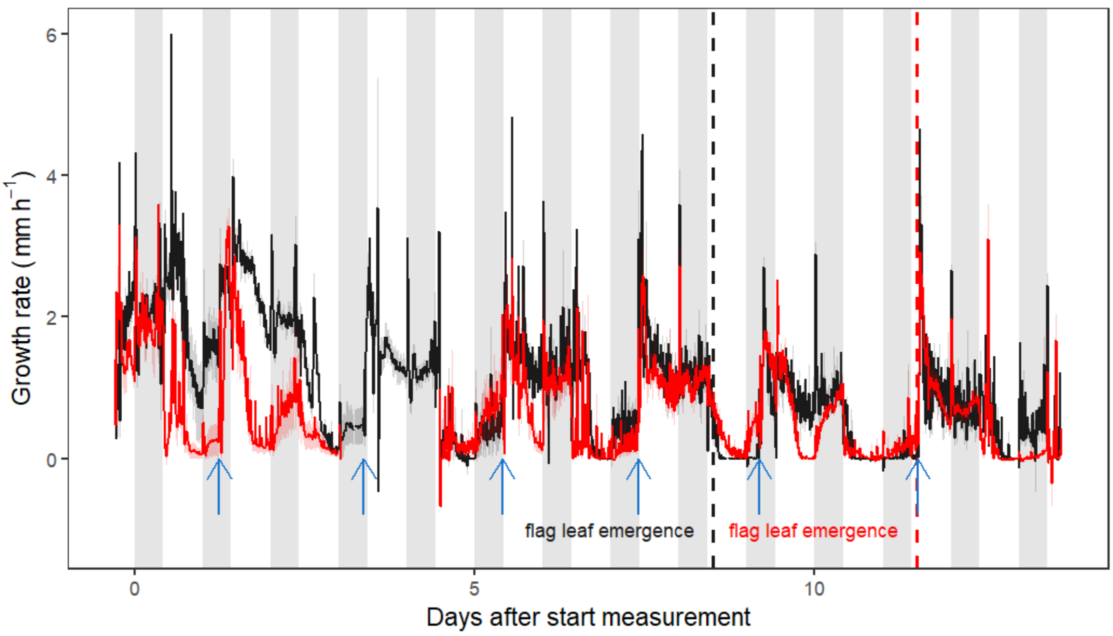

Figure 9. Growth rate of well-watered plants (black line, n = 4) and drought-treated plants (red line, n = 4). Grey and light red bands indicate standard error. Blue arrows represent the time of watering: control and drought-treated plants received 500 mL and 150 mL, respectively, each time, except on day 8, when drought-treated plants were watered 300 mL to avoid wilting. The black and red vertical dashed line indicate the moment when 50% of the flag leaves of well-watered plants and drought-treated plants were fully emerged, respectively. Grey areas in the background indicate the absence of light.

4. Discussion

4.1 Environmental conditions do not affect sensor calibration, while extreme events may impact continuous measurements

Not many studies measuring leaf elongation using the ‘sensor and pulley system’ mention sensor calibration. One exception is the study of Fricke et al. (2004), which briefly cites the use of a micrometer. Our results show that a theoretical calibration based on the circumference of the pulley and the maximum measured voltage difference of the sensor yields an on average 4.33±0.25% too small calibration value (Table 2) and thus – if applied – will underestimate leaf growth. Our results also suggest that a sensor-specific calibration is preferred over a common calibration for all sensors (Table 1). Calibration values may differ due to a deviation in the circumference of the pulley (which in our case was the main reason for the deviation of sensor number 7) or due to differences in the maximum voltage across the sensor. Also, the calibration process is affected by the angle between the calibrator and the pulley, which is to be expected according to classical trigonometry rules. This means that if, in practice, it proves impossible to place the leaf to be measured perpendicular below the pulley, it will influence the accuracy of the measurement if not accounted for. Fortunately, calibration values and measurements can easily be corrected according to classic trigonometric rules (Table 1, 2, Figure 2). This also showed that other possible error-introducing factors, such as extra slip of the thread on the pulley, did not play a role in our experiment.

Although environmental conditions did not affect sensor calibration (Table 1), this was not entirely true for its influence on the sensor system (logger + sensor + pulley + Kevlar thread) (Figure 3C) when tested under extreme (freezing) conditions. Large environmental shocks, with vapour pressure deficit (VPD) changing rapidly from near zero to over 1 kPa or *vice versa*, caused variation in the measurements, with a large deviation with one sensor (sensor 3), probably caused by logger interference, especially since sensor 4, connected to the same logger, showed a similar (but less pronounced) deviation pattern. In practice, however, environmental changes are less extreme, and growth does not occur under freezing conditions. Often environmental conditions are similar to the conditions of the second treatment and do not seem to have a major impact on RDT measurements (Figures 3B,D). The measured deviation remained limited, and all sensors showed a similar pattern, likely caused by the shrinking and expanding of the Kevlar thread under the influence of changing VPD (Sadok et al., 2007). These results are in line with but not equal to Parent et al. (2009), who reported no effect of VPD on RDT measurements at all.

4.2 Calibrated RDT sensors accurately measure growth and are robust against physical disturbances

Manual leaf growth measurements indicate that the calibration of individual RDT sensors with the height gauge provided accurate growth measurements when the measurement process is not disturbed (Figure 4). The R^2-value (0.99) is much higher than the one obtained by Sadok et al. (2007) ($R^2 = 0.72$). However, the two values cannot be compared, as Sadok et al. (2007) compared manual measurements of elongation rate of cut leaves with RDT-attached leaves. It is possible that the tension of the RDT imposed on the leaf influences the elongation process, or that destructive measurements of leaf length do not represent *in vivo* conditions.

Even when the measurement process was disturbed and the thread was touched (red dots in Figure 5), possible influences did not last long. Slightly higher measurement points were alternated with slightly lower ones, cancelling each other out, and average growth rate was subsequently recorded accurately. The fact that the measurement points after the disturbances in Figure 5 were lower than before was not due to the disturbances themselves but rather to the water regime, as the wheat plants were watered 24 hours before the disturbances and thus leaf turgor and leaf growth was higher before.

4.3 Complex architecture of the wheat plant affects the interpretation of sensor data

Given the accurate calibration and validation of the RDT sensors on wheat leaves in experiments 1 and 2, the difference between manual and RDT measurements during the first three days of the experiment (Figures 6 and 8) cannot be explained by inaccurate monitoring of the sensor system, but rather by the architectural dynamics of the wheat shoot. When manually measuring flag leaf growth based on the visible part of the leaf, the leaf sheath that it is enclosed by (the sheath of the penultimate leaf in this case) grows independently of the flag leaf (Figure 10A to B) as it is attached to a lower node. Any growth of that enclosing leaf sheath is thus masking growth of the flag leaf itself. Manual measurements therefore may underestimate the true leaf growth:

$$\begin{aligned} &\mathit{manual\ measurement} \\ &\qquad = \mathit{growth\ flag\ leaf\ blade} \\ &\qquad + \mathit{growth\ flag\ leaf\ sheath} - \mathit{growth\ penultimate\ leaf\ sheath} \end{aligned} \tag{3}$$

In contrast, when growth of the flag leaf is measured by the sensor, it cannot be assumed that only growth of the leaf blade and sheath are contributing to the measurements. After all, the leaf sheath is attached to a node. And as the internode below and the subsequent internodes grow, this node, and thus also the leaf attached to it, are pushed upwards. The sensor therefore registers growth of both the leaf (blade + sheath) and the subsequent supporting structures (Figure 10). Sensor measurements overestimate the true leaf growth when supporting structures grow:

$$\begin{aligned} &\mathit{RDT\ measurements} \\ &\qquad = \mathit{growth\ flag\ leaf\ blade} + \mathit{growth\ flag\ leaf\ sheath} \\ &\qquad + \mathit{growth\ penultimate\ internode} + \mathit{growth\ lower\ internodes} \end{aligned} \tag{4}$$

As a result, the growth rate measured by an RDT sensor can only be termed LER (leaf elongation rate) when it is known that the subsequent internodes have stopped elongating.

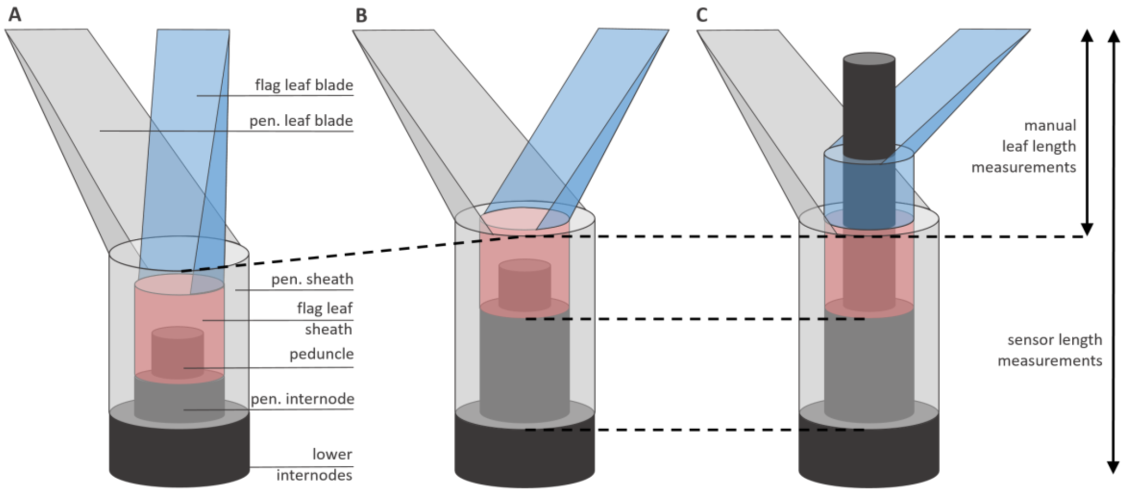

Figure 10. Stepwise representation of the growth of a wheat plant and its flag leaf (blade in blue and sheath in red). The grey coloured leaf grows independently of the flag leaf and can mask part of the growth measurements of the flag leaf. A to B) Before flag leaf appearance, mostly the flag leaf blade elongates, but the penultimate leaf sheath can still elongate, as well as the penultimate internode. B) flag leaf appearance. B to C) After flag leaf appearance, mostly the flag leaf sheath elongates (Figure 7), as well as the peduncle, which grows independently. Arrows on the right show the difference between the manual and sensor measurements. The ear is not depicted for simplicity, but develops on top of the peduncle. Pen.: penultimate.

Although Salah and Tardieu (1995) clearly described to take the possible growth of supporting plant parts into account when measuring leaf blade growth of maize (with an LVDT), this reflection gradually disappeared in later papers (e.g., Seneweera et al., 2005; Sadok et al., 2007; Mahdit et al., 2011). The difference between manual and RDT measurements found in our study serves as a reminder that, when measuring growth rate on monocotyledons with a shoot architecture such as maize and wheat with transducers like RDT or LVDT, it is important to take possible growth of supporting parts into account. Turc et al. (2016) followed this protocol when measuring the elongation of maize silks.

When considering the difference between both growth measurement methods (Eq 3 – Eq 4), this falls down to:

$$\Delta growth = -\,growth\ penultimate\ leaf\ sheath - growth\ penultimate\ internode - growth\ lower\ internodes \quad (5)$$

Because the difference between the two measurement methods disappeared from six days before full flag leaf emergence of well-watered plants (which is three days after the start of the experiment) (Figure 8), we can conclude that after this point the penultimate leaf sheath and penultimate and lower internodes stopped elongating. From this point onwards, the RDT sensors measured true LER of the flag leaf in both well-watered and drought-treated plants. Both the growth of the flag leaf sheath and blade are comprised in this elongation rate, although manual data suggests that the leaf sheath mainly elongated when the blade stopped elongating (Figure 7).

4.4 Drought as a major driver of flag leaf growth dynamics

Despite the influence of the internode and penultimate leaf sheath elongation in the first three days of the experiment, statements on the impact of drought on flag leaf growth can be made as drought had no effect on the relative differences between manual and RDT measurements throughout the experiment (Figure 8). The reduced flag leaf growth of drought-treated wheat plants (-36%) (Figure 6), as a result of a reduction in cell division and cell expansion, is consistent with other recent research on wheat flag leaf growth dynamics. In Boussakouran et al. (2019), flag leaf length of drought plants was 30% lower than in irrigated plants, and Mickky et al. (2019) showed that flag leaf specific area was reduced under drought in all ten tested wheat varieties, although such decreases were non-significant at $p \leq 0.05$.

Drought had the largest effect in the beginning of the experiment (Figure 9), which matches the period of leaf blade growth (Figure 7). This opens the suggestion that leaf blade growth is more sensitive to drought than growth of the sheath. In this regard, it has been reported that plants might have lower leaf specific area under drought to reduce transpiration (Poorter et al., 2009). Figure 7 does however also show a reduced flag leaf sheath elongation due to drought stress. Our data does therefore not fully support this hypothesis. The lower LER in plants under droughts stress is reported to be compensated partly by an increase in leaf elongation duration, for example by Nelissen et al. (2018) in maize. While this still needs to be established for wheat, Coussement et al. (2018) confirmed this through a conceptual model of turgor time, showing that growth follows turgor time, which only increases when turgor exceeds a threshold value. Growth slows down when final organ dimensions are reached. If turgor is not reached due to for example drought stress, turgor time does not increase and growth is prolonged on the thermal time and real time scale. Although we did not measure until flag leaves were fully grown, there was no sign of prolonged flag leaf growth in drought plants since growth rates of both drought-treated and well-watered plants were slowing down at the end of the measurement period (Figure 9).

Drought also had a major impact on daily growth rate dynamics with the rate of drought-treated plants decreasing more and earlier during the day, being at its lowest at the end of the day and partially recovering at night and reaching its highest value at predawn. To our knowledge, our study is the first to examine growth rate time courses of wheat flag leaves under stable environmental conditions (changing only at day-night transitions), isolating and highlighting the impact of soil water status. Earlier research on LER time courses (Salah and Tardieu, 1997; Caldeira et al., 2014; Tardieu et al., 2014), performed on the sixth leaf of maize, mimicked daily patterns (with maximum values of light intensity, VPD and air temperature around midday) which led to different daily time courses compared to our experiment, because LER is very responsive to changing environmental conditions (Munns et al., 2000). Salah and Tardieu (1997), for example, found that while well-watered plants were roughly following air temperature, drought-stressed plants followed the opposite pattern, with minimal LER at midday, probably following leaf turgor dynamics. When these authors corrected for changes in air temperature, LER in maize in both well-watered and drought-stressed plants decreased during daytime with increasing VPD and transpiration, resulting in opposite diurnal trends between LER and biomass acquisition and, as in our study, nightly LER being maximal at the end of the night (Caldeira et al., 2014; Tardieu et al., 2014).

Conclusions

Our study shows that calibration of RDT sensors with a height gauge results in accurate and robust measurements of growth rates and drought dynamics in monocotyledons, with only extreme changes in environmental conditions negatively impacting the sensors. When using these sensors to measure growth rates in monocotyledons, growth of the supporting structures must be taken into account as well, as not only leaf blade elongation is registered. Further research with the RDT sensor on flag leaf growth dynamics and its underlying mechanisms on different wheat cultivars have the potential to improve yield, since morpho-physiological traits such as flag leaf length have been emphasized in the literature as important secondary traits for wheat breeding under drought stress.

Acknowledgments

We acknowledge the contribution of Dr. Hans Van de Put for performing the thread screening experiment. The authors thank Philip Deman, Geert Favyts, and Erik Moerman for their help with the technical setup of the experiment.

Data availability

The data presented in this study and related R-scripts are available on request from the corresponding author

Funding

This work was funded by Flanders' Food and VLAIO (Flanders Innovation & Entrepreneurship) as part of the SpaceBakery project (HBC.2019.0100), and by the Special Research Fund (BOF) of Ghent University, Belgium, through the basic infrastructure funding 01B04515 and BOF20/BAS/043 granted to KS.

Author contributions

K. Steppe, together with S. Verbeke, conceptualised the ideas. S. Dequeker and S. Verbeke performed the experiments together. S. Dequeker analysed the data with the support of S. Verbeke and K. Steppe. The manuscript was written by S. Dequeker and S. Verbeke with the support of K. Steppe, who supervised the project.

References

Acevedo, E., Hsiao, T. C., Henderson, D. W., 1971. Immediate and subsequent growth responses of maize leaves to changes in water status. Plant Physiol., https://doi.org/10.1104/pp.48.5.631

Avramova, V., Meziane, A., Bauer, E., Blankenagel, S., Eggels, S., Gresset, S., et al., 2019. Carbon isotope composition, water use efficiency, and drought sensitivity are controlled by a common genomic segment in maize. Theor. Appl. Genet., https://doi.org/10.1007/s00122-018-3193-4

Biswal, A.K., Kohli, A., 2013. Cereal flag leaf adaptations for grain yield under drought: knowledge status and gaps. Mol. Breed., https://doi.org/10.1007/s11032-013-9847-7

Boussakouran, A., Sakar, E.H., El Yamani, M., Rharrabti, Y., 2019. Morphological Traits Associated with Drought Stress Tolerance in Six Moroccan Durum Wheat Varieties Released Between 1984 and 2007. J. Crop Sci. Biotechnol., 22, 345–353.

Boyer, J., 1970. Leaf enlargement and metabolic rates in corn, soybean, and sunflower at various leaf water potentials. Plant physiol., https://doi.org/10.1104/pp.46.2.233

Bultynck, L., Ter Steege, M. W., Schortemeyer, M., Poot, P., Lambers, H., 2004. From individual leaf elongation to whole shoot leaf area expansion: a comparison of three Aegilops and two Triticum species. Ann. Bot., https://doi.org/10.1093/aob/mch110

Caldeira, C. F., Bosio, M., Parent, B., Jeanguenin, L., Chaumont, F., Tardieu, F., 2014. A hydraulic model is compatible with rapid changes in leaf elongation under fluctuating evaporative demand and soil water status. Plant Physiol., https://doi.org/10.1104/pp.113.228379

Chenu, K., Chapman, S. C., Hammer, G. L., Mclean, G., Salah, H. B. H., Tardieu, F., 2008. Short-term responses of leaf growth rate to water deficit scale up to whole-plant and crop levels: an integrated modelling approach in maize. Plant Cell Environ., https://doi.org/10.1111/j.1365-3040.2007.01772.x

Coussement, J., De Swaef, T., Lootens, P., Roldán-Ruiz, I., Steppe K., 2018. Introducing turgor-driven growth dynamics into functional-structural plant models. Ann. Bot., https://doi.org/10.1093/aob/mcx144

Fricke, W., Akhiyarova, G., Veselov, D., Kudoyarova, G., 2004. Rapid and tissue-specific changes in ABA and in growth rate in response to salinity in barley leaves. J. Exp. Bot., https://doi.org/10.1093/jxb/erh117

Granier, C., Inzé, D., Tardieu, F., 2000. Spatial distribution of cell division rate can be deduced from that of p34cdc2 kinase activity in maize leaves grown at contrasting temperatures and soil water conditions. Plant Physiol., https://doi.org/10.1104/pp.124.3.1393

IPCC, 2022. Climate Change 2022: Impacts, Adaptation, and Vulnerability. Contribution of Working Group II to the Sixth Assessment Report of the Intergovernmental Panel on Climate Change In: Pörtner, H.-O., Roberts, D.C., Tignor, M., Poloczanska, E.S., Mintenbeck, K., Alegría, A., Craig, M., Langsdorf, S., Löschke, S., Möller, V., Okem, A., Rama, B. (eds.). Cambridge University Press. Cambridge University Press, Cambridge, UK and New York, NY, USA, 3056 pp.

Lacube, S., Fournier, C., Palaffre, C., Millet, E.J., Tardieu, F., Parent, B., 2017. Distinct controls of leaf widening and elongation by light and evaporative demand in maize. Plant Cell Environm. https://doi.org/10.1111/pce.13005

Mahdid, M., Kameli, A., Ehlert, C., Simonneau, T., 2011. Rapid changes in leaf elongation, ABA, and water status during the recovery phase following application of water stress in two durum wheat varieties differing in drought tolerance. Plant Physiol. Biochem., https://doi.org/10.1016/j.plaphy.2011.08.002

Matos, D. A., Cole, B. J., Whitney, I. P., MacKinnon, K. J. M., Kay, S. A., Hazen, S. P., 2014. Daily changes in temperature, not the circadian clock, regulate growth rate in Brachypodium distachyon. PLoS One, https://doi.org/10.1371/journal.pone.0100072

Mickky, B., Aldesuquy, H., Elnajar, M., 2019. Drought-induced change in yield capacity of ten wheat cultivars in relation to their vegetative characteristics at heading stage. Physiol. Mol. Biol. Plants, https://doi.org/10.1007/s12298-019-00705-0

Mielewczik, M., Friedli, M., Kirchgessner, N., Walter, A. 2013. Diel leaf growth of soybean: a novel method to analyze two-dimensional leaf expansion in high temporal resolution based on a marker tracking approach (Martrack Leaf). Plant methods, 9: 30.

Munns, R., Passioura, J. B., Guo, J., Chazen, O., Cramer, G. R., 2000. Water relations and leaf expansion: importance of time scale. J. Exp. Bot., https://doi.org/10.1093/jexbot/51.350.1495

Nelissen, H., Sun, X. H., Rymen, B., Jikumaru, Y., Kojima, M., Takebayashi, Y., et al., 2018. The reduction in maize leaf growth under mild drought affects the transition between cell division and cell expansion and cannot be restored by elevated gibberellic acid levels. Plant Biotechnol. J., https://doi.org/10.1111/pbi.12801

Nyce, D. S., 2016. Position sensors. John Wiley & Sons, Hoboken, New Jersey, p8-13.

Ong, C. K., 1983. Response to temperature in a stand of pearl millet (Pennisetum typhoides S. & H.) 4. Extension of individual leaves. J. Exp. Bot., https://doi.org/10.1093/jxb/34.12.1731

Parent, B., Hachez, C., Redondo, E., Simonneau, T., Chaumont, F., Tardieu, F., 2009. Drought and abscisic acid effects on aquaporin content translate into changes in hydraulic conductivity and leaf growth rate: a trans-scale approach. Plant physiol., https://doi.org/10.1104/pp.108.130682

Parent, B., Suard, B., Serraj, R., Tardieu, F., 2010a. Rice leaf growth and water potential are resilient to evaporative demand and soil water deficit once the effects of root system are neutralized. Plant Cell Environ., https://doi.org/10.1111/j.1365-3040.2010.02145.x

Parent, B., Turc, O., Gibon, Y., Stitt, M., Tardieu, F., 2010b. Modelling temperature-compensated physiological rates, based on the co-ordination of responses to temperature of developmental processes. J. Exp. Bot., https://doi.org/10.1093/jxb/erq003

Poiré, R., Wiese-Klinkenberg, A., Parent, B., Mielewczik, M., Schurr, U., Tardieu, F., Walter, A., 2010. Diel time-courses of leaf growth in monocot and dicot species: endogenous rhythms and temperature effects. J. Exp. Bot., https://doi.org/10.1093/jxb/erq049

Poorter, H., Niinemets, Ü., Poorter, L., Wright, I. J., Villar, R., 2009. Causes and consequences of variation in leaf mass per area (LMA): a meta-analysis. New Phyt., https://doi.org/10.1111/j.1469-8137.2009.02830.x

Reymond, M., Muller, B., Tardieu, F., 2004. Dealing with the genotype× environment interaction via a modelling approach: a comparison of QTLs of maize leaf length or width with QTLs of model parameters. J. Exp. Bot., https://doi.org/10.1093/jxb/erh200

Saab, I. N., Sharp, R. E., 1989. Non-hydraulic signals from maize roots in drying soil: inhibition of leaf elongation but not stomatal conductance. Planta, https://doi.org/10.1007/BF00397586

Sadok, W., Naudin, P., Boussuge, B., Muller, B., Welcker, C., Tardieu, F., 2007. Leaf growth rate per unit thermal time follows QTL-dependent daily patterns in hundreds of maize lines under naturally fluctuating conditions. Plant Cell Environ., https://doi.org/10.1111/j.1365-3040.2006.01611.x

Salah, H. B. H., Tardieu, F., 1995. Temperature affects expansion rate of maize leaves without change in spatial distribution of cell length. Analysis of the coordination between cell division and cell expansion. Plant Physiol., https://doi.org/10.1104/pp.109.3.861

Salah, H. B. H., Tardieu, F. 1997. Control of leaf expansion rate of droughted maize plants under fluctuating evaporative demand (a superposition of hydraulic and chemical messages?). Plant Physiol., https://doi.org/10.1104/pp.114.3.893

Seneweera, S. P., Conroy, J. P., 2005. Enhanced leaf elongation rates of wheat at elevated CO2: is it related to carbon and nitrogen dynamics within the growing leaf blade? Environ. Exp. Bot., https://doi.org/10.1016/j.envexpbot.2004.07.002

Tardieu, F., Parent, B., Caldeira, C. F., Welcker, C., 2014. Genetic and physiological controls of growth under water deficit. Plant Physiol., https://doi.org/10.1104/pp.113.233353

Tardieu, F., Simonneau, T., Parent, B., 2015. Modelling the coordination of the controls of stomatal aperture, transpiration, leaf growth, and abscisic acid: update and extension of the Tardieu–Davies model. J. Exp. Bot., https://doi.org/10.1093/jxb/erv039

Turc, O., Bouteille, M., Fuad-Hassan, A., Welcker, C., Tardieu, F., 2016. The growth of vegetative and reproductive structures (leaves and silks) respond similarly to hydraulic cues in maize. New Phytol., https://doi.org/10.1111/nph.14053

Van Eeuwijk, F. A., Bustos-Korts, D., Millet, E. J., Boer, M. P., Kruijer, W., Thompson, A., et al., 2019. Modelling strategies for assessing and increasing the effectiveness of new phenotyping techniques in plant breeding. Plant Sci., https://doi.org/10.1016/j.plantsci.2018.06.018

Welcker, C., Boussuge, B., Bencivenni, C., Ribaut, J.M., Tardieu, F., 2007. Are source and sink strengths genetically linked in maize plants subjected to water deficit? A QTL study of the responses of leaf growth and of anthesis-silking interval to water deficit. J. Exp. Bot., https://doi.org/10.1093/jxb/erl227